Isolation of Novel Lignans, Heteroclitins F and G, from the Stems of *Kadsura heteroclita*, and Anti-lipid Peroxidative Actions of Heteroclitins A—G and Related Compounds in the *in Vitro* Rat Liver Homogenate System

Xiu-Wei YANG,[a] Hirotsugu MIYASHIRO,[a] Masao HATTORI,*[,a] Tsuneo NAMBA,[a] Yasuhiro TEZUKA,[a] Tohru KIKUCHI,[a] Dao-Feng CHEN,[b] Guo-Jun XU,[b] Toshihiko HORI,[c] Michael EXTINE,[c] and Hiroshi MIZUNO[d]

Research Institute for Wakan-Yaku, Toyama Medical and Pharmaceutical University,[a] 2630 Sugitani, Toyama 930-01, Japan, China Pharmaceutical University,[b] 24 Tong Jia Xiang, Nanjing, China, Research and Development Division, Rigaku Industrial Corporation,[c] Akishima, Tokyo 196, Japan and National Institute of Agrobiological Resources,[d] Tsukuba Science City, Ibaragi 305, Japan. *Received January 7, 1992*

From the stems of *Kadsura heteroclita*, two new lignans named heteroclitins F and G were isolated and their structures were determined by various spectroscopic means including an X-ray diffraction method. Dibenzocyclo-octadiene type lignans and related compounds isolated from the stems of *K. heteroclita*, potently inhibited the lipid peroxidation in the rat liver homogenate stimulated by Fe^{2+}–ascorbic acid, CCl_4–reduced form of nicotinamide adenine dinucleotide phosphate (NADPH) and adenosine 5′-diphosphate–NADPH.

Keywords anti-lipid peroxidation; dibenzocyclo-octadiene type lignan; heteroclitin; *Kadsura heteroclita*; Schizandraceae; X-ray diffraction

The stems of *Kadsura heteroclita* (ROXB.) CRAIB. (Schizandraceae) have been used in traditional Chinese medicine for the treatment of gastric and duodenal ulcers, acute and chronic gastroenteritis, dysmenorrhea, post-partum abdominal pain and trauma. Some triterpenes have been hitherto reported as regards the constituents of this plant.[1-3]

In the course of our chemical and pharmacological studies on the stems of *K. heteroclita*, we have isolated five new dibenzocyclo-octadiene type lignans named heteroclitins A—E[4] and found anti-lipid peroxidative effects of the extract and its major constituent, kadsurin, on CCl_4-intoxicated mice.[5]

In the present paper, we describe the isolation and characterization of two new lignans from the stems of *K. heteroclita*, and the effects of heteroclitins A—G and related compounds on the lipid peroxidation in the rat liver homogenate stimulated by Fe^{2+}–ascorbic acid, CCl_4–reduced form of nicotinamide adenine dinucleotide phosphate (NADPH) and adenosine 5′-diphosphate (ADP)–NADPH.

Results and Discussion

Structures of Heteroclitins F and G An EtOH extract of the stems of *K. heteroclita* was partitioned between 90% MeOH and hexane. The 90% MeOH-soluble portion was further extracted with $CHCl_3$. Repeated column chromatography (CC) of the hexane-soluble and $CHCl_3$–soluble fractions followed by preparative thin layer chromatography (prep. TLC) led to the isolation of two new lignans named heteroclitins F and G, together with the previously reported lignans [kadsurin (**1**), interiorin (**2**) and heteroclitins A—E (**3**—**7**)] (see Chart 1), and steroids (β-sitosterol and β-sitosten-3-one). The structures of these compounds were determined by spectroscopic means as follows.

Heteroclitin F (**8**), $[\alpha]_D^{25}$ +261.2°, was obtained as colorless powder and its molecular formula was determined to be $C_{27}H_{30}O_{10}$ by high-resolution mass spectrometry (HRMS). The ultraviolet (UV) spectrum showed λ_{max} at 212 nm, quite different from those of previously isolated dibenzocyclo-octadiene type lignans, heteroclitins A—E (Table I).[4] The proton nuclear magnetic resonance

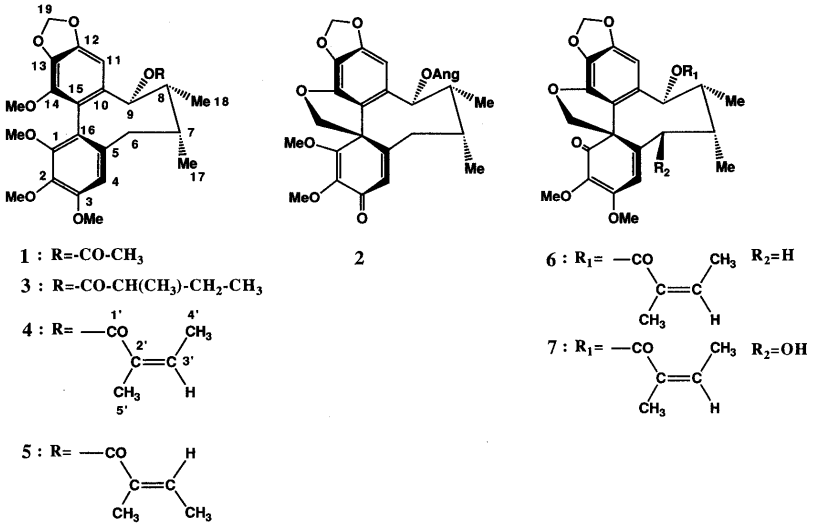

Chart 1. Structures of Heteroclitins A—E and Related Compounds

(^{1}H-NMR) spectrum showed the presence of an angeloyl group, two methoxy groups (δ_H 3.61, 3.67), one methylenedioxy group (δ_H 5.99, 6.01, AB quartet, $J=1.2$ Hz), two *sec*-methyl groups (δ_H 1.10, 1.16), two aromatic/vinyl protons (δ_H 6.07, 6.45), two methine protons (δ_H 2.01, 2.13 as two multiplets) and two methylene protons (δ_H 2.47, br t-like and δ_H 4.59, 5.81, each d, $J=10.7$ Hz). In the ^{1}H–^{1}H shift-correlated spectroscopy (^{1}H–^{1}H COSY) experiment, the signal at δ_H 2.01 (H-8) was correlated with the signals at δ_H 1.10 (H_3-18) and 5.57 (H-9), the latter of which was also correlated with the aromatic proton signal at δ_H 6.07 (H-11) possibly in a long-range coupling manner; the signal at δ_H 2.13 (H-7) was correlated with the signals at δ_H 1.16 (H_3-17) and 2.47 (H_2-6). A weak correlation was also observed between the signals of H-7 and H-8. These findings revealed that **8** possessed a partial structure quite similar to that of **6**.

However, **8** contained two more oxygen atoms in the molecule than **6**. The infrared (IR) spectrum showed two carbonyl bands at ν_{max} 1718 and 1740 cm^{-1}, the lower frequency being attributable to a conjugated ester carbonyl in comparison with those of analogous compounds,[4] and the higher frequency to a carbonyl in the 1,2-diketo system or a carbonyl interacted with a polar group at the α position.[6]

TABLE I. UV Spectral Data for Heteroclitins and Related Compounds

Compound	λ_{max} (ε)
Kadsurin (**1**)	219 (27400) 254 (6700) 278 (1800)
Interiorin (**2**)	219 (42800) 245 (16000) 295 (4200)
Heteroclitin A (**3**)	218 (30900) 254 (7600) 278 (2600)
Heteroclitin B (**4**)	219 (56300) 255 (12000) 280 (3000)
Heteroclitin C (**5**)	218 (39700) 254 (8200) 278 (2400)
Heteroclitin D (**6**)	221 (37200) 276 (2200) 332 (4000)
Heteroclitin E (**7**)	219 (43100) 279 (2600) 329 (3400)
Heteroclitin F (**8**)	216 (35800)
Heteroclitin G (**9**)	222 (51500) 288 (3600) 372 (5700)

All UV spectra were measured in MeOH at room temperature.

In the long-range ^{13}C–^{1}H COSY experiment, two doublet signals at δ_H 4.59 (H_a-20) and 5.81 (H_b-20), assignable to a methylene substituted by oxygen (–O–CH_2–), were correlated with the signals of 65.1 (C-16), 118.3 (C-15), 145.3 (C-14), 155.9 (C-5), 184.0 (C-1) (see Table II). These findings indicated that the –O–CH_2– group was attached to C-14 and C-16, forming a spirobenzofuranoid skeleton like in **6**. In addition, two methoxy carbonyl groups were shown to be present by long-range shift

TABLE II. Long-Range ^{13}C–^{1}H COSY Data for Heteroclitin F (**8**)

No.	Carbon chemical shift (δ_C)	Long-range shift-correlated proton signal (δ_H)
1	184.0	4.59 (H_a-20), 5.81 (H_b-20)
2	161.0	3.61 (MeO-2)
3	165.9	3.67 (MeO-3)
4	123.5	2.47 (H_2-6)
5	155.9	2.47 (H_2-6), 4.59 (H_a-20), 5.81 (H_b-20)
6	41.3	1.16 (H_3-17), 6.07 (H-4)
7	35.5	1.10 (H_3-18), 1.16 (H_3-17), 2.01 (H-8), 2.47 (H_2-6), 5.57 (H-9)
8	43.2	1.10 (H_3-18), 1.16 (H_3-17), 2.47 (H-6), 5.57 (H-9)
9	82.8	1.10 (H_3-18), 6.45 (H-11)
10	133.3	5.57 (H-9)
11	103.2	5.57 (H-9)
12	150.8	5.99, 6.01 (H_2-19), 6.45 (H-11)
13	130.6	5.99, 6.01 (H_2-19), 6.45 (H-11)
14	145.3	4.59 (H_a-20), 5.81 (H_b-20)
15	118.3	5.57 (H-9), 5.81 (H_b-20), 6.45 (H-11)
16	65.1	2.47 (H_2-6), 4.59 (H_a-20), 5.81 (H_b-20), 6.07 (H-4)
17	19.9	2.01 (H-8), 2.13 (H-7), 2.47 (H-6)
18	14.4	1.16 (H_3-17), 2.08 (H-8), 5.57 (H-9)
19	102.3	
20	84.5	
MeO-2	52.7	
MeO-3	51.5	
1′	168.1	1.90 (H-4′), 1.93 (H-5′), 5.57 (H-9)
2′	127.9	1.90 (H-4′), 1.93 (H-5′)
3′	139.5	1.90 (H-4′), 1.93 (H-5′)
4′	15.8	
5′	21.4	

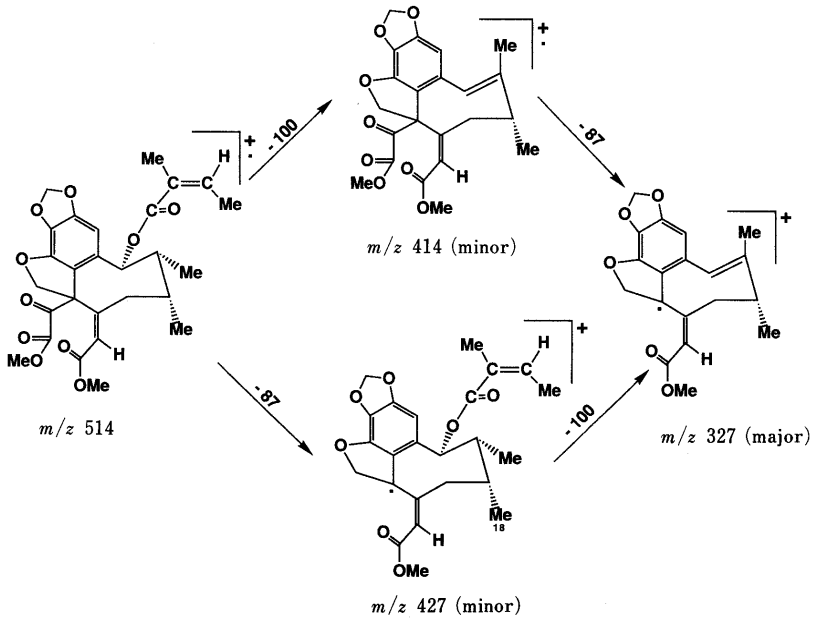

Chart 2. Mass Fragmentation Pattern for Heteroclitin F (**8**)

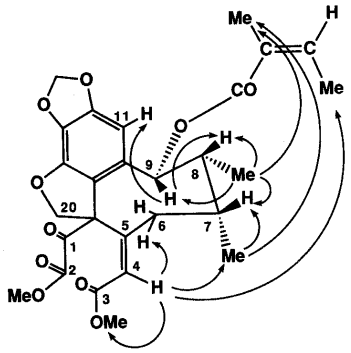

8

Fig. 1. Schematic Illustration of NOE for Heteroclitin F (**8**)

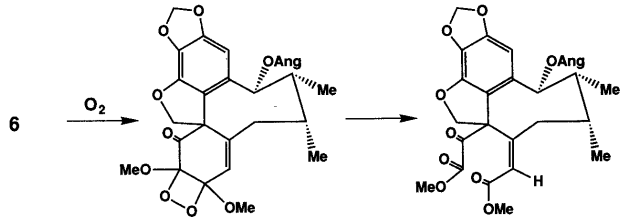

Chart 3. Possible Biogenetic Processes from Heteroclitin D (**6**) to Heteroclitin F (**8**)

correlations of the ^{13}C signals at δ_C 161.0 and 165.9 and the ^1H signals at δ_H 3.61 (MeO) and 3.69 (MeO), respectively. The two methoxycarbonyl groups were consequently located at C-1 and C-4. In the mass spectrum, the fragment ions at *m/z* 427, 414 and 327 (base peak) were indicative of losses of $-CO-COOCH_3$, $(CH_3)CH=CH(CH_3)-CO-O-$ and both groups, respectively, from the molecular ion (*m/z* 514) (Chart 2), which supports the structure **8**.

Appreciable nuclear Overhauser effects (NOE) were observed between the following protons: H-4 *vs.* H-6 and H_3-17, indicating that H-4 and C-6 are *syn*-oriented; H-11 *vs.* H-9; H-9 *vs.* H-8 and H_3-18 (see Fig. 1). However, no NOE enhancement was detected between two methoxy groups on irradiation of either proton signals, indicating that both groups (MeO-2, MeO-3) are not located at the vicinal positions as those in **6** and **7**. Furthermore, two methyl groups of the angeloyl residue were shown to come sufficiently close to interact with H_3-17, H_3-18 and H-4.

The structure was finally determined as **8**, which may be biosynthetically produced from heteroclitin D (**6**) by oxidative cleavage through an intermediate (**6a**) (Chart 3).

Heteroclitin G (**9**), $[\alpha]_D^{25}$ +21.5°, was obtained as yellowish prisms, and its molecular formula was determined as $C_{22}H_{24}O_7$ by HRMS. The ^1H-NMR spectrum showed the presence of three methoxy (δ_H 3.66, 3.80, 4.07), one methylenedioxy (δ_H 5.89, 5.93 as an AB quartet), *tert*-methyl (δ_H 0.90) and *sec*-methyl (δ_H 0.97) groups, a benzylic methylene (δ_H 2.12, 2.83), a methine (δ_H 1.98—2.08 as a multiplet), a benzylic methine substituted by oxygen (δ_H 4.40) and two aromatic protons (δ_H 6.23, 6.74).

In the ^1H–^1H COSY experiment, the multiplet methine signal (H-7) was shift-correlated with *sec*-methyl (H_3-17) and benzylic methylene signals (H_2-6), the latter of which was also shift-correlated with one of the aromatic proton signals (δ_H 6.23; H-4) in a long-range coupling manner.

In addition, appreciable long-range ^{13}C–^1H shift correlations were observed between the signal at δ_C 75.3 (C-16) and the signals at δ_H 4.40 (H-9), 0.90 (H_3-18) and 6.23 (H-4). The long-range shift correlation of C-16 and H_3-18 suggested that C-16 and C-8 were linked. Other

TABLE III. Long-Range ^{13}C–^1H COSY Data for Heteroclitin G (**9**)

Carbon	Chemical shift (δ_C)	Long-range shift-correlated proton signal (δ_H)
1	192.7	
2	135.9	6.23 (H-4), 3.66 (MeO-2)
3	163.2	4.07 (MeO-3)
4	112.8	
5	157.5	2.12 (H_a-6), 2.83 (H_b-6)
6	37.6	0.90 (H_3-18), 0.97 (H_3-17)
7	38.7	0.90 (H_3-18), 0.97 (H_3-17), 2.12 (H_a-6), 2.83 (H_b-6)
8	61.8	0.90 (H_3-18), 0.97 (H_3-17)
9	80.1	0.90 (H_3-18)
10	142.4	4.40 (H-9), 6.74 (H-11)
11	102.1	
12	150.2	5.89, 5.93 (H_2-19)
13	136.5	5.89, 5.93 (H_2-19), 6.74 (H-11)
14	140.1	3.80 (MeO-14)
15	128.6	4.40 (H-9), 6.74 (H-11)
16	75.3	0.90 (H_3-18), 4.40 (H-9), 6.23 (H-4)
17	15.8	
18	10.4	
19	101.4	
MeO-2	60.0	
MeO-3	57.8	
MeO-14	59.6	

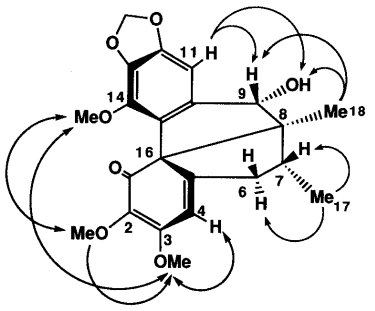

9

Fig. 2. Schematic Illustration of NOE for Heteroclitin G (**9**)

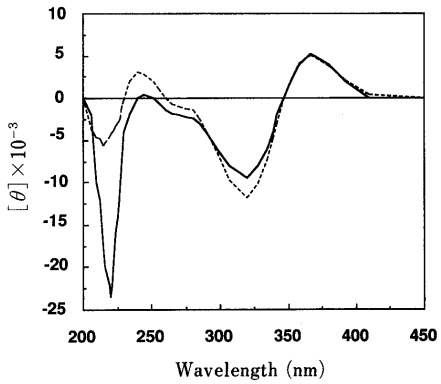

Fig. 3. CD Spectra of Heteroclitins D (**6**) and G (**9**)

The CD spectra were measured in MeOH at 25 °C. ---, heteroclitin D (**6**); ——, heteroclitin G (**9**).

long-range ^{13}C–^{1}H shift correlations were observed for the signal at δ_C 128.6 (C-15) and those of H-11 and H-9; the signal at δ_C 61.8 (C-8) and those of H_3-18 and H_3-17; the singal at δ_C 38.7 (C-7) and those of H_3-17, H_3-18 and H_2-6 (Table III).

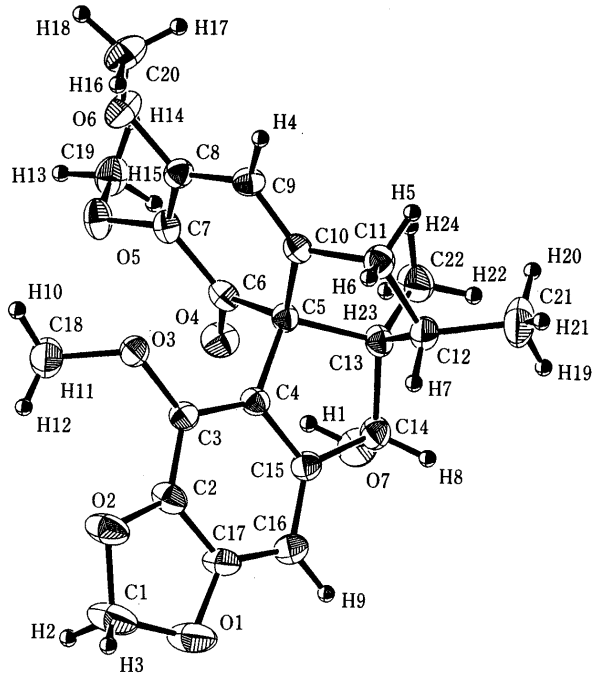

Fig. 4. ORTEP Drawing with Atomic Numbering

Ellipsoids of 30% probability are drawn for the non-H atoms; the H atoms are represented as spheres.

TABLE IV. Fractional Atomic Coordinates and Isotropic Temperature Factors, B_{eq} for Non-H Atoms with Their Estimated Standard Deviations in Parentheses

Atom	x	y	z	B_{eq}
O(1)	0.1464 (4)	0.2419 (1)	0.3997 (3)	6.2 (2)
O(2)	0.0212 (3)	0.3404 (1)	0.3931 (3)	5.4 (1)
O(3)	0.0154 (2)	0.4363 (1)	0.1557 (2)	3.6 (1)
O(4)	0.0463 (3)	0.3230 (1)	−0.2017 (3)	4.3 (1)
O(5)	−0.1456 (2)	0.4214 (1)	−0.2294 (2)	4.2 (1)
O(6)	−0.0802 (2)	0.5519 (1)	−0.1894 (3)	4.6 (1)
O(7)	0.2689 (3)	0.2436 (1)	−0.1590 (3)	4.9 (1)
C(1)	0.0395 (6)	0.2763 (2)	0.4625 (4)	6.2 (3)
C(2)	0.0891 (4)	0.3337 (2)	0.2732 (4)	3.7 (2)
C(3)	0.0897 (3)	0.3778 (2)	0.1621 (3)	3.0 (1)
C(4)	0.1746 (3)	0.3610 (2)	0.0565 (3)	2.9 (1)
C(5)	0.1918 (3)	0.3988 (2)	−0.0806 (3)	2.7 (1)
C(6)	0.0696 (3)	0.3826 (2)	−0.1638 (3)	3.1 (1)
C(7)	−0.0219 (3)	0.4374 (2)	−0.1860 (3)	3.2 (1)
C(8)	0.0116 (3)	0.5043 (2)	−0.1596 (3)	3.2 (1)
C(9)	0.1394 (3)	0.5225 (2)	−0.1102 (4)	3.2 (1)
C(10)	0.2231 (3)	0.4742 (2)	−0.0700 (3)	2.9 (1)
C(11)	0.3649 (4)	0.4833 (2)	−0.0349 (4)	3.7 (2)
C(12)	0.4261 (3)	0.4116 (2)	−0.0471 (4)	3.8 (2)
C(13)	0.3266 (3)	0.3675 (2)	−0.1295 (4)	3.3 (2)
C(14)	0.3268 (4)	0.2935 (2)	−0.0718 (4)	3.8 (2)
C(15)	0.2509 (4)	0.3015 (2)	0.0608 (4)	3.3 (1)
C(16)	0.2487 (4)	0.2571 (2)	0.1719 (4)	3.9 (2)
C(17)	0.1664 (4)	0.2753 (2)	0.2756 (4)	3.9 (2)
C(18)	−0.1220 (4)	0.4262 (2)	0.1729 (5)	5.5 (2)
C(19)	−0.1615 (4)	0.4139 (2)	−0.3717 (4)	4.6 (2)
C(20)	−0.0588 (4)	0.6228 (2)	−0.1537 (5)	5.3 (2)
C(21)	0.5641 (4)	0.4125 (2)	−0.1028 (6)	6.9 (3)
C(22)	0.3454 (5)	0.3726 (2)	−0.2833 (4)	4.9 (2)

Furthermore, NOE was observed among the following protons: H-11 *vs.* H-9, HO-9; H_3-18 *vs.* H-9 and HO-9; H_3-17 *vs.* H-6 and H-7; H-4 *vs.* MeO-3; MeO-2 *vs.* MeO-14 and MeO-3 (Fig. 2). The circular dichroism (CD) spectrum of **9** showed a positive band at 376 nm and negative bands at 221 and 320 nm, quite similar to those of **6** (Fig. 3), indicating that both compounds possess an *S*-configuration.

The structure and stereochemistry of **9** were finally established by a single-crystal X-ray analysis using the direct method. As shown in Fig. 4, the structure was quite in agreement with that deduced by NMR spectroscopy. The ORTEP[7] drawings of **9** shows thermal ellipsoids

TABLE V. Bond Distances (Å) for Non-H Atoms with Their Estimated Standard Deviations in Parentheses

Atom	Atom	Distance	Atom	Atom	Distance
O1	C1	1.420 (5)	C5	C6	1.522 (5)
O1	C17	1.387 (4)	C5	C10	1.503 (4)
O2	C1	1.429 (4)	C5	C13	1.581 (4)
O2	C2	1.365 (4)	C6	C7	1.434 (5)
O3	C3	1.369 (4)	C7	C8	1.367 (5)
O3	C18	1.429 (5)	C8	C9	1.438 (5)
O4	C6	1.240 (4)	C9	C10	1.330 (5)
O5	C7	1.370 (4)	C10	C11	1.500 (5)
O5	C19	1.403 (4)	C11	C12	1.532 (5)
O6	C8	1.350 (4)	C12	C13	1.554 (5)
O6	C20	1.438 (4)	C12	C21	1.513 (5)
O7	C14	1.418 (5)	C13	C14	1.544 (5)
C2	C3	1.382 (4)	C13	C22	1.513 (5)
C2	C17	1.383 (5)	C14	C15	1.515 (5)
C3	C4	1.385 (4)	C15	C16	1.384 (5)
C4	C5	1.534 (4)	C16	C17	1.362 (5)
C4	C15	1.396 (4)			

TABLE VI. Bond Angles (°) for Non-H Atoms with Their Estimated Standard Deviations in Parentheses

Atom	Atom	Atom	Angle	Atom	Atom	Atom	Angle
C1	O1	C17	105.6 (3)	O6	C8	C7	115.9 (3)
C1	O2	C2	104.7 (3)	O6	C8	C9	122.4 (3)
C3	O3	C18	115.3 (3)	C7	C8	C9	121.7 (3)
C7	O5	C19	115.8 (3)	C8	C9	C10	120.7 (3)
C8	O6	C20	119.9 (3)	C5	C10	C9	122.0 (3)
O1	C1	O2	107.9 (3)	C5	C10	C11	109.7 (3)
O2	C2	C3	127.8 (3)	C9	C10	C11	127.4 (3)
O2	C2	C17	110.8 (3)	C10	C11	C12	105.7 (3)
C3	C2	C17	121.3 (3)	C11	C12	C13	105.8 (3)
O3	C3	C2	123.3 (3)	C11	C12	C21	113.5 (3)
O3	C3	C4	120.7 (3)	C13	C12	C21	115.7 (3)
C2	C3	C4	116.0 (3)	C5	C13	C12	101.8 (3)
C3	C4	C5	127.2 (3)	C5	C13	C14	104.5 (3)
C3	C4	C15	121.6 (3)	C5	C13	C22	112.6 (3)
C5	C4	C15	111.1 (3)	C12	C13	C14	108.9 (3)
C4	C5	C6	105.7 (2)	C12	C13	C22	113.1 (3)
C4	C5	C10	115.6 (3)	C14	C13	C22	114.9 (3)
C4	C5	C13	100.3 (3)	O7	C14	C13	114.7 (3)
C6	C5	C10	114.4 (3)	O7	C14	C15	111.5 (3)
C6	C5	C13	118.4 (3)	C13	C14	C15	102.4 (3)
C10	C5	C13	102.1 (2)	C4	C15	C14	110.2 (3)
O4	C6	C5	120.7 (3)	C4	C15	C16	122.1 (3)
O4	C6	C7	121.6 (3)	C14	C15	C16	127.7 (3)
C5	C6	C7	117.5 (3)	C15	C16	C17	115.4 (3)
O5	C7	C6	118.7 (3)	O1	C17	C2	108.3 (3)
O5	C7	C8	120.4 (3)	O1	C17	C16	128.0 (3)
C6	C7	C8	120.9 (3)	C2	C17	C16	123.6 (3)

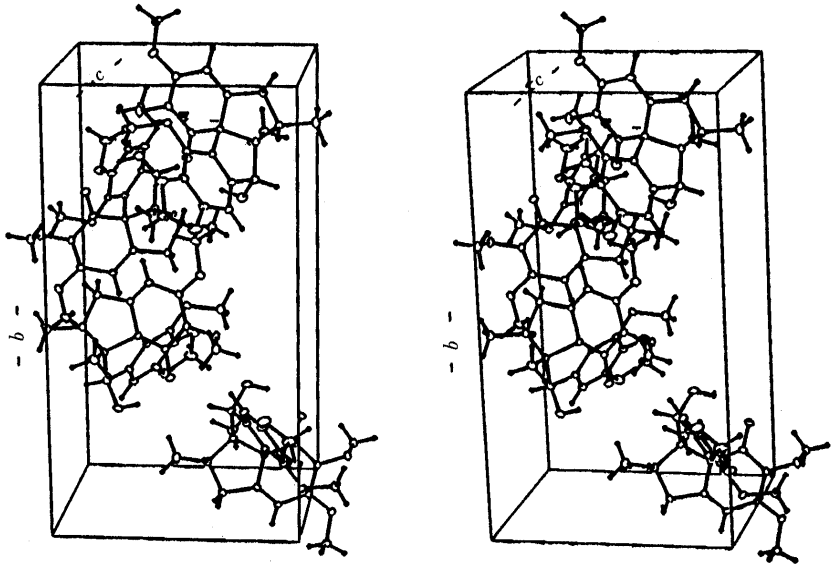

Fig. 5. Stereoview of the Unit-Cell Packing
Ellipsoids of 10% probability are drawn for the non-H atoms.

of non-H atoms and the atomic numbering. The final positional parameters and equivalent isotropic parameters are given in Table IV. Interatomic bond distances and angles are listed in Tables V and VI. An intramolecular hydrogen bond O–H···O is observed [O4···O7= 2.782(4) Å, O4···H1 = 1.95(5) Å, O4–H1–O7 = 155(5)°].

Figure 5 shows the molecular packing of **9**. Intermolecular contacts are mainly based on hydrophobic interaction. Short contact is observed only between O2 and H15–C19 of the neighboring molecule (symmetry operation: x, y, $z+1$) [O2···H15 = 2.48 Å, O2···C19 = 3.284(5) Å].

Heteroclitins F (**8**) and G (**9**) are new natual products of C-2, 3 *seco*- and C-8,16 linked-dibenzocyclo-octadiene type lignans, respectively.

Anti-lipid Peroxidative Actions of Heteroclitins A—G and Related Compounds As has been reported previously,[5] successive administration of a 95% EtOH extract or its major component, kadsurin (**1**), in mice significantly inhibited the CCl_4-induced formation of thiobarbituric acid reactive substances (TBA-RS), lipid conjugated diene and fluorescent products in the liver tissue. The anti-lipid peroxidative effect of the extract was partly due to an appreciable increase(s) of superoxide dismutase (SOD)-like enzyme(s). Since dibenzocyclo-octadiene lignans have been reported to have a free radical scavenging or anti-oxidative property,[8,9] we investigated the anti-lipid peroxidative effects of the isolated compounds in the *in vitro* system. Lipid peroxidation in the rat liver homogenate is stimulated by the addition of $FeCl_2$–ascorbic acid, CCl_4–NADPH or ADP–NADPH. The $FeCl_2$–ascorbic acid-stimulated lipid peroxidation mainly proceeds through non-enzymatic processes, while the CCl_4–NADPH- or ADP–NADPH-stimulated lipid peroxidation proceeds through enzymatic processes by the action of cytochrome P-450.

In the presence of $FeCl_2$ and ascorbic acid, the TBA-RS level as an indicator of lipid peroxidation in the rat liver homogenate appreciably increased as shown in Table VII.

TABLE VII. Effects of Heteroclitins A—G and Related Compounds on the $FeCl_2$–Ascorbic Acid, CCl_4–NADPH and ADP–NADPH-Stimulated Lipid Peroxidation in the Rat Liver Homogenate

Compounds	Concentration $\times 10^{-4}$ M	TBA-RS (nmol)/g wet wt of the liver tissue		
		$FeCl_2$–ascorbic acid	CCl_4–NADPH	ADP–NADPH
Normal control		67.6±2.67[b]	78.8±0.70[b]	93.3±0.65[b]
Treated control[a]		110.9±1.26	115.3±1.13	135.9±3.01
Heteroclitin A	1.0	98.6±0.42[b]	115.0±1.82	110.2±1.73[b]
	2.0	65.3±1.37[b]	103.1±2.38[b]	86.0±0.88[b]
Heteroclitin B	1.0	102.3±1.37[c]	117.1±3.16	95.1±1.05[b]
	2.0	90.9±1.95[b]	112.0±2.40	90.7±0.84[b]
Heteroclitin C	1.0	93.3±3.99[b]	116.2±2.46	109.5±9.68[c]
	2.0	92.4±2.65[b]	110.2±2.38	92.7±3.24[b]
Heteroclitin D	1.0	88.2±1.05[b]	113.3±0.61	107.0±9.28[b]
	2.0	63.1±1.19[b]	110.9±3.00	96.1±2.72[b]
Heteroclitin E	1.0	99.7±1.67[c]	111.8±2.40	102.0±6.41[b]
	2.0	75.3±4.23[b]	108.1±1.11[c]	85.8±2.46[b]
Heteroclitin F	1.0	103.9±0.55	116.9±2.10	100.9±4.66[b]
	2.0	74.6±2.67[b]	109.3±0.70[c]	90.2±4.67[b]
Heteroclitin G	1.0	95.5±4.09[b]	115.9±2.08	98.7±2.22[b]
	2.0	86.5±1.16[b]	115.2±2.46	85.7±0.97[b]
Kadsurin	1.0	101.5±1.37	100.5±1.37[b]	98.9±0.81[b]
	2.0	92.9±5.36[b]	99.0±0.72[b]	85.5±1.20[b]
Interiorin	1.0	89.1±1.16[b]	110.9±1.95	107.4±4.40[b]
	2.0	86.7±1.50[b]	105.8±0.85[b]	93.6±1.34[b]
DL-α-Tocopherol	1.0	79.2±2.17[b]	110.2±0.63[b]	111.4±7.10[b]
	2.0	78.6±1.92[b]	98.7±0.97[b]	94.2±2.12[b]

Values are means±S.E. of 4 determinations. *a*) Treated with $FeCl_2$–ascorbic acid, CCl_4–NADPH or ADP–NADPH. *b*) $p<0.01$; *c*) $p<0.05$ *vs.* the respective controls treated with $FeCl_2$–ascorbic acid, CCl_4–NADPH and ADP–NADPH.

However, the addition of various dibenzocyclo-octadiene type lignans at concentrations of 1.0—2.0 × 10^{-4} M inhibited the formation of TBA-RS. Of the compounds tested, heteroclitins A (**3**) and D (**6**) at 2.0 × 10^{-4} M most potently inhibited the Fe^{2+}–ascorbic acid-stimulated lipid peroxidation, the TBA-RS levels being equivalent to or less than a control level. Anti-lipid peroxidative potencies of these compounds at this concentration were stronger than that of DL-α-tocopherol (positive control).

In a CCl_4–NADPH-stimulated lipid peroxidation, kadsurin (**1**), interiorin (**2**) and heteroclitins A (**3**), E (**7**)

and F (**8**) at a concentration of 2.0×10^{-4} M significantly lowered the TBA-RS levels in the rat liver homogenate. Of these compounds, kadsurin (**1**) inhibited the lipid peroxidation with a potency equivalent to that of DL-α-tocopherol.

In an ADP–NADPH-stimulated lipid peroxidation, most of the compounds inhibited the formation of TBA-RS. The TBA-RS levels were lowered to a control level by the addition of 2.0×10^{-4} M kadsurin (**1**), interiorin (**2**) and heteroclitins A (**3**), C (**5**) and E (**7**)—G (**9**).

These findings indicated that the dibenzocyclo-octadiene type lignans isolated from the stems of *K. heteroclita* had free radical scavenging or anti-oxidant action to inhibit lipid peroxidation. Therefore, the *K. heteroclita* extract activates anti-lipid peroxidative enzymes such as SOD in the liver by chronic administration in mice as reported previously,[5] and its constituents absorbed from the gastrointestinal tract may also directly inhibit lipid peroxidation in the liver by terminating the lipid oxidation processes induced by free radicals or active oxygens.

Experimental

Apparatus Melting points were determined on a Yanagimoto micro-melting point apparatus and are uncorrected. IR spectra were taken on a Hitachi 260-01 IR spectrometer. ^{1}H-NMR and ^{13}C-NMR spectra were measured with a JEOL GX-400 (^{1}H, 400 MHz, ^{13}C, 100 MHz) spectrometer using tetramethylsilane (TMS) as an internal standard. UV spectra were measured with a Shimadzu UV-260 spectrophotometer (Shimadzu, Kyoto). Electron impact mass spectra (EIMS) and HRMS were measured with a JMS DX-300 mass spectrometer. Optical rotations were measured with a JASCO DIP-4 automatic polarimeter at 25 °C. CD spectra were recorded on a JASCO J-500 spectropolarimeter equipped with a JASCO DP-500 data processor.

Chromatography Wakogel C-200 was used for CC. TLC was performed on Merck Kieselgel 60 F_{254} plates (Merck Co., Darmstadt, Germany) with a solvent system of hexane–acetone–benzene (14 : 5 : 1). Spots on the plate were observed under UV light and visualized by spraying with an anisaldehyde–H_2SO_4 reagent followed by heating.

Material The stems of *K. heteroclita* were collected in Feng-Qing County, Yunnan Province, China, in August of 1989, and its botanical source was confirmed by G.-J. Xu and the voucher specimens were deposited at the Herbarium of Materia Medica of China Pharmaceutical University and the Museum of Materia Medica of Toyama Medical and Pharmaceutical University.

Chemicals TBA, sodium dodecyl sulfate (SDS), carbon tetrachloride (CCl_4), NADPH, L(+)-ascorbic acid and anhydrous $FeCl_2$ were purchased from Wako Pure Chemical Industries Ltd. (Osaka, Japan). DL-α-Tocopherol (vitamin E) and ADP were obtained from Nacalai Tesque Co. (Kyoto, Japan) and Sigma Chemicals Co. (St. Louis, MO, U.S.A.) respectively. Other chemicals were of special reagent grade. Ultra pure water was used in all bioassays.

Extraction and Fractionation As has been previously reported,[4] the dried and pulverized stems of *K. heteroclita* (4 kg) were extracted five times with 95% EtOH (7.0 l) under reflux for 8 h. The combined solutions were evaporated *in vacuo* to give a residue (114 g), which was suspended in 90% MeOH (1.5 l), followed by extraction with hexane to give a hexane-soluble fraction (36.5 g). The remaining methanolic solution was evaporated to give a residue (82.5 g), which was suspended in water (1.0 l) and extracted with $CHCl_3$ (2.0 ml × 5) to give a $CHCl_3$-soluble fraction (48.1 g).

The hexane-soluble fraction was applied to a silica gel column (3.8 cm i.d. × 80 cm), which was successively eluted with hexane containing increasing amounts of $CHCl_3$. Fractions eluted with hexane–$CHCl_3$ (10 : 2.5) were subjected to repeated CC and prep. TLC to yield kadsurin (**1**; 1.14 g), heteroclitin A (**3**; 32 mg), heteroclitin B (**4**; 78 mg), heteroclitin C (**5**; 114 mg), β-sitosterol and β-sitosten-3-one. Similarly, fractions eluted with hexane–$CHCl_3$ (10 : 5) gave heteroclitin F (**8**, 19 mg), interiorin (**2**; 459 mg) and heteroclitin D (**6**; 499 mg), and a fraction eluted with $CHCl_3$–EtOAc (8 : 2) gave heteroclitin G (**9**, 81 mg).

The $CHCl_3$-soluble fraction was chromatographed on a silica gel column (3.8 cm i.d. × 80 cm) with hexane–$CHCl_3$ (1 : 1) and $CHCl_3$. The $CHCl_3$ eluate was repeatedly chromatographed to give heteroclitin G (**9**, 319 mg) and heteroclitin E (**7**; 27 mg).

Heteroclitin F (8) Colorless powder, $[\alpha]_D^{25}$ +261.2° (MeOH, c=0.33). CD (MeOH, $c = 2.0 \times 10^{-4}$ g/ml) (nm): +6500 (328). UV λ_{max}^{MeOH} nm (ε): 216 (35800). IR ν_{max}^{KBr} cm^{-1}: 1740 (C=O), 1718 (conjugated ester C=O), 1650, 1620 (aromatic). EIMS m/z: 514 $[M]^+$, 427 $[M-C_3H_3O_3]^+$, 414 $[M-C_5H_8O_2]^+$, 327 $[M-C_3H_3O_3-C_5H_9O_2]^+$. HRMS: Found, m/z: 514.1814 $[M]^+$, Calcd for $C_{27}H_{30}O_{10}$: 514.1839. ^{1}H-NMR (400 MHz, $CDCl_3$) δ: 1.10 (3H, d, J=7.3 Hz, H_3-18), 1.16 (3H, d, J=7.6 Hz, H_3-17), 1.90 (3H, dq, $J_{4',5'}$=1.5 Hz, $J_{3'4'}$=7.3 Hz, H_3-4'), 1.93 (3H, m, H_3-5'), 1.99—2.04 (1H, m, H-8), 2.11—2.14 (1H, m, H-7), 2.47 (2H, br t-like, H_2-6), 3.61 (3H, s, MeO-2), 3.67 (3H, s, MeO-3), 4.59 (1H, d, J=10.7 Hz, H_a-20), 5.57 (1H, br d, $J_{6,7}$=1.5 Hz, H-9), 5.81 (1H, d, J=10.7 Hz, H_b-20), 5.99, 6.01 (2H, ABq, J=1.2 Hz, H_2-19), 6.03—6.07 (1H, m, H-3'), 6.07 (1H, s, H-4), 6.45 (1H, s, H-11).

Heteroclitin G (9) Yellowish prisms from EtOAc; mp 214—215 °C; $[\alpha]_D^{25}$ +21.5° (MeOH, c=0.91). CD (MeOH, $c = 2.0 \times 10^{-4}$ g/ml) (nm): −23400 (221), −2000 (270), −9400 (320), +5200 (376). UV λ_{max}^{MeOH} nm (ε): 222 (51500), 288 (3600), 372 (5700). IR ν_{max}^{KBr} nm^{-1}: 3340 (OH), 1662, 1605 (aromatic). EIMS m/z: 400 $[M]^+$. HRMS: Found, m/z: 400.1368 $[M]^+$, Calcd for $C_{22}H_{24}O_7$: 400.1369. ^{1}H-NMR (400 MHz, $CDCl_3$) δ: 0.90 (3H, s, H_3-17), 0.97 (3H, d, J=6.7 Hz, H_3-18), 1.98—2.08 (1H, m, H-7), 2.12 (1H, ddd, J=1.5, 8.2, 18.0 Hz, H_a-6), 2.83 (1H, ddd, J=2.4, 10.1, 18.0 Hz, H_b-6), 3.66, 3.80, 4.07 (each 3H, each s, MeO-1,2,14), 4.40 (1H, d, J=12.2 Hz, H-9), 5.07 (1H, d, J=12.2 Hz, HO-9), 5.89 (1H, d, J=1.2 Hz, Ha-19), 5.93 (1H, d, J=1.2 Hz, H_b-19), 6.23 (1H, br s, H-4), 6.74 (1H, s, H-11).

β-Sitosterol EIMS m/z: 414 $[M]^+$. The ^{1}H- and ^{13}C-NMR spectra agreed with those of an authentic sample.

β-Sitosten-3-one EIMS m/z: 412 $[M]^+$. IR ν_{max}^{KBr} cm^{-1}: 1670 (conj. C=O). The ^{1}H- and ^{13}C-NMR spectra were identical with those of an authentic sample.

X-Ray Crystallographic Analysis of Heteroclitin G (9) Yellow prismatic crystals were grown from an EtOAc solution of **9** by slow evaporation. The cell dimensions were determined by a least-squares refinement of 20 reflections in the range of $55° < 2\theta < 60°$ measured on a Rigaku AFC5R four-circle diffractometer equipped with a rotating anode (Ni-filtered Cu$K\alpha$, 40 kV, 200 mA). Crystal data: $C_{22}H_{24}O_7$, M_r=400.43, orthorhombic, $P2_12_12_1$, a=10.231(1), b=19.430(1), c=9.739(1) Å, V=1936.1(3) Å^3, Z=4, D_X=1.374 g cm^{-3}, λ(Cu$K\alpha$)=1.54178 Å, μ=8.09 cm^{-1}, $F(000)$=848. Intensity data were collected at 20 °C within $2\theta_{max}$=122° ($0<h<11$, $0<k<22$, $0<l<11$) by the ω–2θ scan technique (scan speed was 4°/min in ω and scan range in ω was 0.6°+0.5 tan θ). Background was measured for 3.75 s on either side of the peak. Three standard reflections were monitored every 100 reflections. Of the 1734 reflections, 1490 reflections with $I > 3.0\ \sigma(I)$ were treated as observed. The intensities were corrected for Lorentz and polarization effects, and secondary extinction (coefficient: 0.2135E-0.4). Decay corrections were applied, but no absorption correction was made.

Structure Determination and Refinement The structure was solved by direct method.[10,11] The non-hydrogen atoms were refined anisotropically. The hydroxy hydrogen atom (H1) was refined isotropically. The remaining hydrogen atoms were included in calculated positions, assuming idealized geometries, and were not refined. Full-matrix least-squares refinement was performed to minimize $\Sigma w(|F_O|-|F_C|)^2$ where $w = 4F_O^2/\sigma^2(F_O^2)$ and $\sigma^2(F_O^2) = [S^2(C+R^2B)+(pF_O^2)^2]/Lp^2$ (S=scan rate, C=total integrated peak count, R=ratio of scan time to background counting time, B=total background count, Lp=Lorentz and polarization factors, and p=0.03). Final cycles of least-squares refinement yielded R=0.035 and wR=0.043 for 1490 reflections. Maximum and minimum peaks on the final difference Fourier map produced 0.14 and −0.18 eÅ^{-3}, respectively. Neutral atom scattering factors were taken from Cromer and Waber.[12] Anomalous dispersion effects were included in F_C; the values for $\Delta f'$ and $\Delta f''$ were those of Cromer.[13] All calculations were performed using the TEXSAN software package.[14] A complete list of X-ray structure data was deposited to the Cambridge Crystallographic Data Centre.

Preparation of Rat Liver Homogenate Male Sprague-Dawley rats weighing 150 g (6 weeks of age) were killed by decapitation, and their liver tissues were quickly removed. A 2 g portion of liver tissues was sliced and homogenized with 10 ml of 150 mM KCl–Tris–HCl buffer (pH 7.2) and then centrifuged at 500 × g for 10 min. The supernatant was used for the study of *in vitro* lipid peroxide formation.

$FeCl_2$–Ascorbic Acid-Stimulated Lipid Peroxidation According to the methods of Yoden *et al.*[15] and Kimuya *et al.*,[16] a mixture containing 0.5 ml of the liver homogenate, 0.1 ml of 150 mM Tris–HCl buffer (pH 7.2),

0.2 ml of 6 mM ascorbic acid, 0.1 ml of 4 mM $FeCl_2$ and 0.1 ml of a test compound solution was incubated for 1 h at 37 °C. After incubation, 0.5 ml of 0.1 N HCl, 0.5 ml of 0.9% SDS and 0.5 ml of H_2O were added to 0.5 ml of the above incubation mixture. The mixture was vigorously shaken and then 2 ml of 0.5% TBA were added, followed by heating for 30 min on a boiling water bath. After cooling, 5 ml of BuOH were added and the mixture was vigorously shaken. The BuOH phase was separated by centrifugation and the optical density at 532 nm was measured. The TBA-RS produced was calculated with a calibration curve prepared from authentic malondialdehyde (MDA) and lipid peroxide values were expressed as nmol of TBA-RS per g of liver tissue.

CCl_4–NADPH-Stimulated Lipid Peroxidation A mixture containing 0.5 ml of liver homogenate, 0.2 ml of a test compound solution and 0.19 ml of 100 mM phosphate buffer (pH 7.4) was preincubated for 15 min at 37 °C. The reaction was then started by adding 0.1 ml of 2 mM NADPH and 10 μl of a CCl_4 solution (0.9 μl of CCl_4 was diluted with EtOH to a volume of 10 μl), and incubated for 20 min at 37 °C. The TBA-RS produced was determined by the method as described above.

ADP–NADPH-Stimulated Lipid Peroxidation A mixture containing 0.5 ml of the liver homogenate, 0.1 ml of 150 mM Tris–HCl (pH 7.2) and 0.2 ml of a test compound solution was preincubated for 15 min at 37 °C. 0.1 ml of 4 mM NADPH and 0.1 ml of 40 mM ADP were then added and the mixture was incubated for 1 h at 37 °C. The TBA-RS produced was determined as described above.

Statistical Analysis The data are expressed as means ± S.E. and statistical significance was evaluated by the method of Dunnett.

References and Notes

1) K. Kangouri, T. Miyoshi, A. Kawashima, A. Ikeda, T. Mizutani, S. Omura, and H. Xue, *Planta Med.*, **55**, 297 (1989).
2) L. Li, H. Hue, D. Ge, K. Kangouri, T. Miyoshi, and S. Omura, *Planta Med.*, **55**, 300 (1989).
3) L. Li, H. Hue, K. Kangouri, A. Kawashima, and S. Omura, *Planta Med.*, **55**, 548 (1989).
4) D. Chen, G. Xu, X. Yang, M. Hattori, Y. Tezuka, T. Kikuchi, and T. Namba, *Phytochemistry*, **31**, 629 (1992).
5) X. Yang, M. Hattori, T. Namba, D. Chen, and G. Xu, *Chem. Pharm. Bull.*, **40**, 406 (1992).
6) L. J. Bellamy, "Advances in Infrared Group Frequencies," Richard Clay Ltd., Bungay, Suffolk, 1968, p. 146.
7) C. K. Johnson, "ORTEP II," Report ORNL-5138, Oak Ridge National Laboratory, Oak Ridge, TN, 1976.
8) Y. Kiso, M. Tohkin, H. Hikino, Y. Ikeya, and H. Taguchi, *Planta Med.*, **51**, 333 (1985).
9) H. Lu and G. Lu, *Chem. Biol. Interactions*, **78**, 77 (1991).
10) C. J. Gilmore, MITHRIL, an integrated direct methods computer program, *J. Appl. Cryst.*, **17**, 42 (1984).
11) P. T. Beurskens, DIRDIF, direct methods for difference structures an automatic procedure for phase extension and refinement of different structure factors, Technical Report 1984/1 Crystallography Laboratory, Toernooiveld, 6525 Ed Nijmegen, Netherlands.
12) D. T. Cromer and J. T. Waber, "International Tables for X-Ray Crystallography," Vol. IV, The Kynoch Press, Birmingam, Table 2. 2A, 1974.
13) D. T. Cromer, "International Tables for X-Ray Crystallography," Vol. IV, The Kynoch Press, Birmingham, Table 2.3.1, 1974.
14) TEXSAN, TEXRAY, structure analysis package, MSC, 3200A Research Forest Drive, The Woodlands, TX, 1985.
15) K. Yoden, T. Iio, and T. Tabata, *Yakugaku Zasshi*, **100**, 553 (1980).
16) Y. Kimuya, M. Kubo, T. Tani, S. Arichi, and H. Okuda, *Chem. Pharm. Bull.*, **29**, 2610 (1981).